

# Probing New Physics via the $B_s^0 \rightarrow \mu^+ \mu^-$ Effective Lifetime

Kristof De Bruyn,<sup>1</sup> Robert Fleischer,<sup>1,2</sup> Robert Knegjens,<sup>1</sup> Patrick Koppenburg,<sup>1</sup> Marcel Merk,<sup>1,2</sup>  
Antonio Pellegrino,<sup>1</sup> and Niels Tuning<sup>1</sup>

<sup>1</sup>*Nikhef, Science Park 105, NL-1098 XG Amsterdam, Netherlands*

<sup>2</sup>*Department of Physics and Astronomy, Vrije Universiteit Amsterdam, NL-1081 HV Amsterdam, Netherlands*  
(Received 12 April 2012; published 25 July 2012)

We have recently seen new upper bounds for  $B_s^0 \rightarrow \mu^+ \mu^-$ , a key decay to search for physics beyond the standard model. Furthermore a nonvanishing decay width difference  $\Delta\Gamma_s$  of the  $B_s$  system has been measured. We show that  $\Delta\Gamma_s$  affects the extraction of the  $B_s^0 \rightarrow \mu^+ \mu^-$  branching ratio and the resulting constraints on the new physics parameter space and give formulas for including this effect. Moreover, we point out that  $\Delta\Gamma_s$  provides a new observable, the effective  $B_s^0 \rightarrow \mu^+ \mu^-$  lifetime  $\tau_{\mu^+ \mu^-}$ , which offers a theoretically clean probe for new physics searches that is complementary to the branching ratio. Should the  $B_s^0 \rightarrow \mu^+ \mu^-$  branching ratio agree with the standard model, the measurement of  $\tau_{\mu^+ \mu^-}$ , which appears feasible at upgrades of the Large Hadron Collider experiments, may still reveal large new physics effects.

DOI: 10.1103/PhysRevLett.109.041801

PACS numbers: 13.20.He, 12.60.-i

**Introduction.**—Thanks to the Large Hadron Collider (LHC) at CERN we have entered a new era of particle physics. One of the most promising processes for probing the quark-flavor sector of the standard model (SM) is the rare decay  $B_s^0 \rightarrow \mu^+ \mu^-$ . In the SM, it originates only from box and penguin topologies, and the  $CP$ -averaged branching ratio is predicted to be [1]

$$\text{BR}(B_s \rightarrow \mu^+ \mu^-)_{\text{SM}} = (3.2 \pm 0.2) \times 10^{-9}, \quad (1)$$

where the error is fully dominated by nonperturbative QCD effects determined through lattice studies. The most stringent experimental upper bound on this branching ratio is given by  $\text{BR}(B_s \rightarrow \mu^+ \mu^-) < 4.5 \times 10^{-9}$  at the 95% confidence level (C.L.) [2].

In the presence of new physics (NP), there may be additional contributions through new particles in the loops or new contributions at the tree level, which are forbidden in the SM (see Ref. [1] and references therein).

A key feature of the  $B_s$ -meson system is  $B_s^0$ - $\bar{B}_s^0$  mixing. This quantum mechanical effect gives rise to time-dependent oscillations between the  $B_s^0$  and  $\bar{B}_s^0$  states. In contrast to the  $B_d$  system, we expect a sizable difference  $\Delta\Gamma_s \equiv \Gamma_L^{(s)} - \Gamma_H^{(s)}$  between the decay widths of the light and heavy  $B_s$  mass eigenstates [3].

Performing a time-dependent analysis of  $B_s^0 \rightarrow J/\psi \phi$ , the LHCb collaboration has recently reported  $\Delta\Gamma_s = (0.116 \pm 0.019) \text{ ps}^{-1}$  [4], which represents the current most precise measurement of this observable.

As we pointed out in Ref. [5], the sizable  $\Delta\Gamma_s$  complicates the extraction of the branching ratios of  $B_s$ -meson decays, leading to systematic biases as large as  $\mathcal{O}(10\%)$  that depend on the dynamics of the decay at hand.

In the case of the  $B_s^0 \rightarrow \mu^+ \mu^-$  channel, the comparison of the experimentally measured branching ratio with the

theoretical prediction (1) is also affected by this effect, which has so far been neglected in the literature.

It can be included through a measurement of the effective  $B_s^0 \rightarrow \mu^+ \mu^-$  lifetime. As  $B_s^0 \rightarrow \mu^+ \mu^-$  is a rare decay, it turns out that this observable offers another sensitive probe for NP that is theoretically clean and complementary to the branching ratio.

**The general  $B_s \rightarrow \mu^+ \mu^-$  amplitudes.**—The general low-energy effective Hamiltonian for the  $\bar{B}_s^0 \rightarrow \mu^+ \mu^-$  decay can be written as

$$\mathcal{H}_{\text{eff}} = -\frac{G_F}{\sqrt{2}\pi} V_{ts}^* V_{tb} \alpha [C_{10} O_{10} + C_S O_S + C_P O_P + C'_{10} O'_{10} + C'_S O'_S + C'_P O'_P]. \quad (2)$$

Here  $G_F$  is Fermi's constant, the  $V_{qq'}$  are elements of the Cabibbo–Kobayashi–Maskawa (CKM) matrix,  $\alpha$  is the QED fine structure constant, the  $C_i$ ,  $C'_i$  are Wilson coefficients encoding the short-distance physics, while the

$$\begin{aligned} O_{10} &= (\bar{s} \gamma_\mu P_L b)(\bar{\ell} \gamma^\mu \gamma_5 \ell) \\ O_S &= m_b (\bar{s} P_R b)(\bar{\ell} \ell) \\ O_P &= m_b (\bar{s} P_R b)(\bar{\ell} \gamma_5 \ell) \end{aligned} \quad (3)$$

are four-fermion operators with  $P_{L,R} \equiv (1 \mp \gamma_5)/2$ , and  $m_b$  is the  $b$ -quark mass. The  $O'_i$  are obtained from the  $O_i$  by making the replacements  $P_L \leftrightarrow P_R$ . Only operators resulting in nonvanishing contributions to  $\bar{B}_s^0 \rightarrow \mu^+ \mu^-$  are included in (2). In particular, the matrix elements of operators involving the  $\bar{\ell} \gamma^\mu \ell$  vector current vanish.

This notation is similar to Ref. [6], where a model-independent analysis of NP effects in  $b \rightarrow s$  transitions was performed. In the SM, as assumed in (1), only  $C_{10}$  is nonvanishing and given by the real coefficient  $C_{10}^{\text{SM}}$ . An outstanding feature of  $\bar{B}_s^0 \rightarrow \mu^+ \mu^-$  is the sensitivity to

(pseudo-)scalar lepton densities, as described by the  $O_{(P)S}$  and  $O'_{(P)S}$  operators. Their Wilson coefficients are still largely unconstrained and leave ample space for NP.

The hadronic sector of the leptonic  $\bar{B}_s^0 \rightarrow \mu^+ \mu^-$  decay can be expressed in terms of a single, nonperturbative parameter, the  $B_s$ -meson decay constant  $f_{B_s}$  [1].

For the discussion of the observables, we go to the rest frame of the decaying  $\bar{B}_s^0$  meson and distinguish between

the  $\mu_L^+ \mu_L^-$  and  $\mu_R^+ \mu_R^-$  helicity configurations, which we denote as  $\mu_\lambda^+ \mu_\lambda^-$  with  $\lambda = L, R$ . In this notation,  $\mu_L^+ \mu_L^-$  and  $\mu_R^+ \mu_R^-$  are related to each other through a  $CP$  transformation:

$$|(\mu_L^+ \mu_L^-)_{CP}\rangle \equiv (CP)|\mu_L^+ \mu_L^-\rangle = e^{i\phi_{CP}(\mu\mu)}|\mu_R^+ \mu_R^-\rangle, \quad (4)$$

where  $e^{i\phi_{CP}(\mu\mu)}$  is convention-dependent. We then obtain

$$A(\bar{B}_s^0 \rightarrow \mu_\lambda^+ \mu_\lambda^-) = \langle \mu_\lambda^- \mu_\lambda^+ | \mathcal{H}_{\text{eff}} | \bar{B}_s^0 \rangle = -\frac{G_F}{\sqrt{2}\pi} V_{ts}^* V_{tb} \alpha f_{B_s} M_{B_s} m_\mu C_{10}^{\text{SM}} e^{i\phi_{CP}(\mu\mu)(1-\eta_\lambda)/2} [\eta_\lambda P + S], \quad (5)$$

where  $M_{B_s}$  is the  $B_s$  mass,  $\eta_L = +1$  and  $\eta_R = -1$ , and

$$P \equiv \frac{C_{10} - C'_{10}}{C_{10}^{\text{SM}}} + \frac{M_{B_s}^2}{2m_\mu} \left( \frac{m_b}{m_b + m_s} \right) \left( \frac{C_P - C'_P}{C_{10}^{\text{SM}}} \right), \quad (6)$$

$$S \equiv \sqrt{1 - 4 \frac{m_\mu^2}{M_{B_s}^2} \frac{M_{B_s}^2}{2m_\mu} \left( \frac{m_b}{m_b + m_s} \right) \left( \frac{C_S - C'_S}{C_{10}^{\text{SM}}} \right)}. \quad (7)$$

The  $P \equiv |P|e^{i\varphi_P}$  and  $S \equiv |S|e^{i\varphi_S}$  carry, in general, non-trivial  $CP$ -violating phases  $\varphi_P$  and  $\varphi_S$ . However, in the SM, we simply have  $P = 1$  and  $S = 0$  (see also Ref. [6]). The  $\phi_{CP}(\mu\mu)$  factor in (5) originates from using the operator relation  $(CP)^\dagger (CP) = \hat{1}$  and (4) in the leptonic parts of the four-fermion operators.

*The  $B_s \rightarrow \mu^+ \mu^-$  observables.*—For the observables discussed below, we need the

$$A(B_s^0 \rightarrow \mu_\lambda^+ \mu_\lambda^-) = \langle \mu_\lambda^- \mu_\lambda^+ | \mathcal{H}_{\text{eff}}^\dagger | B_s^0 \rangle \quad (8)$$

amplitude. Inserting again  $(CP)^\dagger (CP) = \hat{1}$  into the matrix elements of the four-fermion operators and using both (4) and  $(CP)|B_s^0\rangle = e^{i\phi_{CP}(B_s)}|\bar{B}_s^0\rangle$ , we obtain

$$A(B_s^0 \rightarrow \mu_\lambda^+ \mu_\lambda^-) = -\frac{G_F}{\sqrt{2}\pi} V_{ts} V_{tb}^* \alpha f_{B_s} M_{B_s} m_\mu C_{10}^{\text{SM}} \times e^{i[\phi(B_s) + \phi_{CP}(\mu\mu)(1-\eta_\lambda)/2]} [-\eta_\lambda P^* + S^*], \quad (9)$$

which should be compared with (5). We observe that

$$|A(B_s^0 \rightarrow \mu_{L,R}^+ \mu_{L,R}^-)| = |A(\bar{B}_s^0 \rightarrow \mu_{R,L}^+ \mu_{R,L}^-)|. \quad (10)$$

Following the formalism to describe  $B_s^0$ - $\bar{B}_s^0$  mixing discussed in Ref. [7], we consider the observable

$$\begin{aligned} \xi_\lambda &\equiv -e^{-i\phi_s} \left[ \frac{e^{i\phi_{CP}(B_s)} A(\bar{B}_s^0 \rightarrow \mu_\lambda^+ \mu_\lambda^-)}{A(B_s^0 \rightarrow \mu_\lambda^+ \mu_\lambda^-)} \right] \\ &= -\left[ \frac{+\eta_\lambda P + S}{-\eta_\lambda P^* + S^*} \right]. \end{aligned} \quad (11)$$

Here we have taken into account that the  $B_s^0$ - $\bar{B}_s^0$  mixing phase  $\phi_s \equiv 2 \arg(V_{ts}^* V_{tb})$  is cancelled by the CKM factors in (5) and (9), and that the convention-dependent phase

$\phi_{CP}(B_s)$  is cancelled through (9), whereas  $\phi_{CP}(\mu\mu)$  simply cancels in the amplitude ratio. We notice the relation

$$\xi_L \xi_R^* = \xi_R \xi_L^* = 1. \quad (12)$$

The observables  $\xi_\lambda$  contain all the information for calculating the time-dependent rate asymmetries [7]:

$$\begin{aligned} &\frac{\Gamma(B_s^0(t) \rightarrow \mu_\lambda^+ \mu_\lambda^-) - \Gamma(\bar{B}_s^0(t) \rightarrow \mu_\lambda^+ \mu_\lambda^-)}{\Gamma(B_s^0(t) \rightarrow \mu_\lambda^+ \mu_\lambda^-) + \Gamma(\bar{B}_s^0(t) \rightarrow \mu_\lambda^+ \mu_\lambda^-)} \\ &= \frac{C_\lambda \cos(\Delta M_s t) + S_\lambda \sin(\Delta M_s t)}{\cosh(y_s t / \tau_{B_s}) + \mathcal{A}_{\Delta\Gamma}^\lambda \sinh(y_s t / \tau_{B_s})}. \end{aligned} \quad (13)$$

Here,  $\Delta M_s$  is the mass difference of the heavy and light  $B_s$  mass eigenstates, and

$$y_s \equiv \tau_{B_s} \Delta\Gamma_s / 2 = 0.088 \pm 0.014, \quad (14)$$

where  $\tau_{B_s}$  is the  $B_s$  mean lifetime; the numerical value corresponds to the results of Ref. [4].  $CP$  asymmetries of this kind were considered for  $B_{s,d} \rightarrow \ell^+ \ell^-$  decays (neglecting  $\Delta\Gamma_s$ ) in various NP scenarios in Refs. [8–10].

The observables entering (13) are given as follows:

$$C_\lambda \equiv \frac{1 - |\xi_\lambda|^2}{1 + |\xi_\lambda|^2} = -\eta_\lambda \left[ \frac{2|PS| \cos(\varphi_P - \varphi_S)}{|P|^2 + |S|^2} \right], \quad (15)$$

$$S_\lambda \equiv \frac{2\text{Im}\xi_\lambda}{1 + |\xi_\lambda|^2} = \frac{|P|^2 \sin 2\varphi_P - |S|^2 \sin 2\varphi_S}{|P|^2 + |S|^2}, \quad (16)$$

$$\mathcal{A}_{\Delta\Gamma}^\lambda \equiv \frac{2\text{Re}\xi_\lambda}{1 + |\xi_\lambda|^2} = \frac{|P|^2 \cos 2\varphi_P - |S|^2 \cos 2\varphi_S}{|P|^2 + |S|^2}. \quad (17)$$

It should be emphasized that due to (12)  $\mathcal{S}_{CP} \equiv S_\lambda$  and  $\mathcal{A}_{\Delta\Gamma} \equiv \mathcal{A}_{\Delta\Gamma}^\lambda$  do not depend on the helicity  $\lambda$  of the muons and are theoretically clean observables.

Since it is difficult to measure the muon helicity, we consider the rates

$$\Gamma(B_s^{(-)0}(t) \rightarrow \mu^+ \mu^-) \equiv \sum_{\lambda=L,R} \Gamma(B_s^{(-)0}(t) \rightarrow \mu_\lambda^+ \mu_\lambda^-), \quad (18)$$

and obtain then the  $CP$ -violating rate asymmetry

$$\frac{\Gamma(B_s^0(t) \rightarrow \mu^+ \mu^-) - \Gamma(\bar{B}_s^0(t) \rightarrow \mu^+ \mu^-)}{\Gamma(B_s^0(t) \rightarrow \mu^+ \mu^-) + \Gamma(\bar{B}_s^0(t) \rightarrow \mu^+ \mu^-)} = \frac{\mathcal{S}_{CP} \sin(\Delta M_s t)}{\cosh(y_s t / \tau_{B_s}) + \mathcal{A}_{\Delta\Gamma} \sinh(y_s t / \tau_{B_s})}, \quad (19)$$

where the  $C_\lambda$  terms (15) cancel because of the  $\eta_\lambda$  factor.

It would be most interesting to measure (19) since a nonzero value immediately signaled  $CP$ -violating NP phases. Unfortunately, this is challenging in view of the tiny branching ratio and as tagging, distinguishing between initially present  $B_s^0$  and  $\bar{B}_s^0$  mesons, and time information are required. An expression analogous to (19) holds also for  $B_d \rightarrow \mu^+ \mu^-$  decays.

In practice, the branching ratio

$$\text{BR}(B_s \rightarrow \mu^+ \mu^-)_{\text{exp}} \equiv \frac{1}{2} \int_0^\infty \langle \Gamma(B_s(t) \rightarrow \mu^+ \mu^-) \rangle dt \quad (20)$$

is the first measurement, where the “untagged” rate

$$\begin{aligned} \langle \Gamma(B_s(t) \rightarrow f) \rangle &\equiv \Gamma(B_s^0(t) \rightarrow f) + \Gamma(\bar{B}_s^0(t) \rightarrow f) \\ &\propto e^{-t/\tau_{B_s}} [\cosh(y_s t / \tau_{B_s}) \\ &\quad + \mathcal{A}_{\Delta\Gamma} \sinh(y_s t / \tau_{B_s})] \end{aligned} \quad (21)$$

is introduced [5,11]. The branching ratio (20) is extracted ignoring tagging and time information. As shown in Ref. [5], due to the sizable width difference, the experimental value (20) is related to the theoretical value (calculated in the literature, see, e.g., Refs. [1,6]) through

$$\text{BR}(B_s \rightarrow \mu^+ \mu^-) = \left[ \frac{1 - y_s^2}{1 + \mathcal{A}_{\Delta\Gamma} y_s} \right] \text{BR}(B_s \rightarrow \mu^+ \mu^-)_{\text{exp}}, \quad (22)$$

where

$$\frac{\text{BR}(B_s \rightarrow \mu^+ \mu^-)}{\text{BR}(B_s \rightarrow \mu^+ \mu^-)_{\text{SM}}} = |P|^2 + |S|^2. \quad (23)$$

The  $y_s$  terms in (22) were so far not taken into account in the comparison between theory and experiment.

$\mathcal{A}_{\Delta\Gamma}$  depends sensitively on NP and is hence essentially unknown. Using (14) and varying  $\mathcal{A}_{\Delta\Gamma} \in [-1, +1]$  gives

$$\Delta \text{BR}(B_s \rightarrow \mu^+ \mu^-)|_{y_s} = \pm y_s \text{BR}(B_s \rightarrow \mu^+ \mu^-)_{\text{exp}}, \quad (24)$$

which has to be added to the experimental error of (20).

In the SM, we have  $\mathcal{A}_{\Delta\Gamma}^{\text{SM}} = +1$  and rescale (1) correspondingly by a factor of  $1/(1 - y_s)$ , which results in

$$\text{BR}(B_s \rightarrow \mu^+ \mu^-)_{\text{SM}}|_{y_s} = (3.5 \pm 0.2) \times 10^{-9}, \quad (25)$$

where we have used (14). This is the SM reference for the comparison with the experimental branching ratio (20).

*The effective  $B_s \rightarrow \mu^+ \mu^-$  lifetime.*—With more data available, the decay time information can be included in the analysis. As we pointed out in Ref. [5], the effective lifetime

$$\tau_{\mu^+ \mu^-} \equiv \frac{\int_0^\infty t \langle \Gamma(B_s(t) \rightarrow \mu^+ \mu^-) \rangle dt}{\int_0^\infty \langle \Gamma(B_s(t) \rightarrow \mu^+ \mu^-) \rangle dt} \quad (26)$$

allows the extraction of

$$\mathcal{A}_{\Delta\Gamma} y_s = \frac{(1 - y_s^2) \tau_{\mu^+ \mu^-} - (1 + y_s^2) \tau_{B_s}}{2 \tau_{B_s} - (1 - y_s^2) \tau_{\mu^+ \mu^-}}, \quad (27)$$

yielding

$$\frac{\text{BR}(B_s \rightarrow \mu^+ \mu^-)}{\text{BR}(B_s \rightarrow \mu^+ \mu^-)_{\text{exp}}} = 2 - (1 - y_s^2) \frac{\tau_{\mu^+ \mu^-}}{\tau_{B_s}}. \quad (28)$$

We emphasize that it is crucial to the above equations that  $\mathcal{A}_{\Delta\Gamma}$  in (17) indeed does not depend on the helicities of the muons, i.e.,  $\mathcal{A}_{\Delta\Gamma} \equiv \mathcal{A}_{\Delta\Gamma}^\lambda$ .

Effective lifetimes are experimentally accessible through the decay time distributions of the same samples of untagged events used for the branching fraction measurements, as illustrated by recent measurements of the  $B_s^0 \rightarrow J/\psi f_0$  and  $B_s^0 \rightarrow K^+ K^-$  lifetimes [12] by the CDF and LHCb collaborations: both attained a 7% precision with approximately 500 events, while an even larger sample of  $B_s^0 \rightarrow \mu^+ \mu^-$  events can be collected by the LHC experiments, assuming the standard model value of the  $B_s^0 \rightarrow \mu^+ \mu^-$  branching fraction. Although a precise estimate is beyond the scope of this article, we believe that the data samples that will be collected in the planned high-luminosity upgrades of the CMS and LHCb experiments [13] can lead to a precision of 5% or better.

*Constraints on new physics.*—In order to explore constraints on NP, we introduce

$$\begin{aligned} R &\equiv \frac{\text{BR}(B_s \rightarrow \mu^+ \mu^-)_{\text{exp}}}{\text{BR}(B_s \rightarrow \mu^+ \mu^-)_{\text{SM}}} = \left[ \frac{1 + \mathcal{A}_{\Delta\Gamma} y_s}{1 - y_s^2} \right] (|P|^2 + |S|^2) \\ &= \left[ \frac{1 + y_s \cos 2\varphi_P}{1 - y_s^2} \right] |P|^2 + \left[ \frac{1 - y_s \cos 2\varphi_S}{1 - y_s^2} \right] |S|^2, \end{aligned} \quad (29)$$

where we have used (17) and (22). Using (1) and the upper bound [2] yield  $R < 1.4$ , neglecting the theoretical uncertainty from (1). In the case of  $y_s = 0$ ,  $R$  fixes a circle in the  $|P|$ - $|S|$  plane. For nonzero  $y_s$  values,  $R$  gives ellipses dependent on the phases  $\varphi_{P,S}$ . As these phases are in general unknown, a value of  $R$  results in a circular band. We obtain the upper bounds  $|P|, |S| \leq \sqrt{(1 + y_s)R}$ . As  $R$  does not allow us to separate the  $S$  and  $P$  contributions, there may still be a large amount of NP present, even if the measured branching ratio is close to the SM value.

The measurement of  $\tau_{\mu^+ \mu^-}$  and the resulting observable  $\mathcal{A}_{\Delta\Gamma}$  allows us to resolve this situation, as

$$|S| = |P| \sqrt{\frac{\cos 2\varphi_P - \mathcal{A}_{\Delta\Gamma}}{\cos 2\varphi_S + \mathcal{A}_{\Delta\Gamma}}} \quad (30)$$

fixes a straight line through the origin in the  $|P|$ - $|S|$  plane. In Fig. 1, we show the current  $R$  constraints in the  $|P|$ - $|S|$  plane, and illustrate also those corresponding to (30).

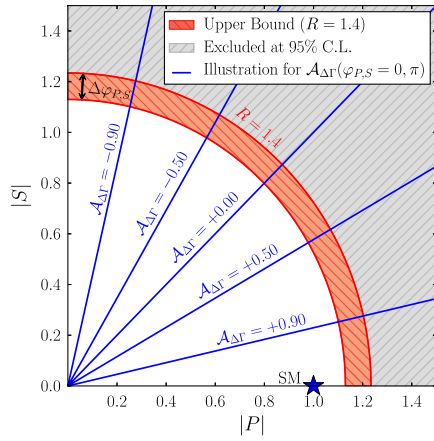


FIG. 1 (color online). Current constraints in the  $|P|$ - $|S|$  plane and illustration of those following from a future measurement of the effective  $B_s \rightarrow \mu^+ \mu^-$  lifetime yielding the  $\mathcal{A}_{\Delta\Gamma}$  observable.

In Fig. 2, we illustrate the situation in the observable space of the  $R$ - $\mathcal{A}_{\Delta\Gamma}$  plane. It will be interesting to complement these model-independent considerations with a scan of popular specific NP models.

Let us finally note that the formalism discussed above can also straightforwardly be applied to  $B_{s(d)} \rightarrow \tau^+ \tau^-$  decays where the polarizations of the  $\tau$  leptons can be inferred from their decay products [10]. This would allow an analysis of (13), where nonvanishing  $C_\lambda$  observables would unambiguously signal the presence of the scalar  $S$  term. Unfortunately, these measurements are currently out of reach from the experimental point of view.

**Conclusions.**—The recently established width difference  $\Delta\Gamma_s$  implies that the theoretical  $B_s^0 \rightarrow \mu^+ \mu^-$  branching ratio in (1) has to be rescaled by  $1/(1 - y_s)$  for the comparison with the experimental branching ratio, giving the SM reference value of  $(3.5 \pm 0.2) \times 10^{-9}$ . The possibility of NP in the decay introduces an additional relative uncertainty of  $\pm 9\%$  originating from  $\mathcal{A}_{\Delta\Gamma} \in [-1, +1]$ .

The effective  $B_s \rightarrow \mu^+ \mu^-$  lifetime  $\tau_{\mu^+ \mu^-}$  offers a new observable. On the one hand, it allows us to take into account the  $B_s$  width difference in the comparison between theory and experiments. On the other hand, it also provides a new, theoretically clean probe of NP. In particular,  $\tau_{\mu^+ \mu^-}$  may reveal large NP effects, especially those related to (pseudo-)scalar  $\ell^+ \ell^-$  densities of four-fermion operators originating from the physics beyond the SM, even in the case that the  $B_s^0 \rightarrow \mu^+ \mu^-$  branching ratio is close to the SM prediction.

The determination of  $\tau_{\mu^+ \mu^-}$  appears feasible with the large data samples that will be collected in the high-luminosity running of the LHC with upgraded experiments and should be further investigated, as this measurement would open a new era for the exploration of  $B_s \rightarrow \mu^+ \mu^-$

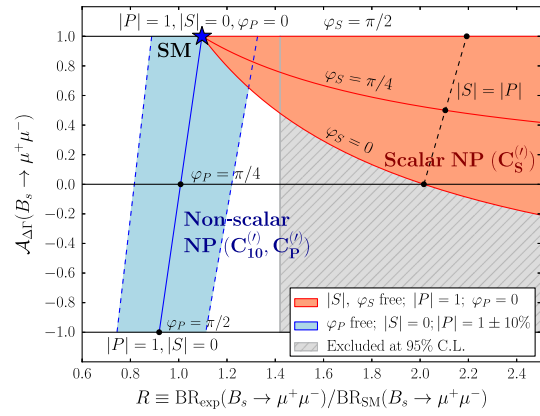


FIG. 2 (color online). Illustration of allowed regions in the  $R$ - $\mathcal{A}_{\Delta\Gamma}$  plane for scenarios with scalar or nonscalar NP contributions.

at the LHC, which may eventually allow the resolution of NP contributions to one of the rarest weak decay processes that nature has to offer.

This work is supported by the Netherlands Organisation for Scientific Research (NWO) and the Foundation for Fundamental Research on Matter (FOM).

- 
- [1] A. J. Buras, Proc. Sci. BEAUTY **2011**, 008 (2011).
  - [2] R. Aaij *et al.* (LHCb Collaboration), *Phys. Rev. Lett.* **108**, 231801 (2012); S. Chatrchyan *et al.* (CMS Collaboration), *J. High Energy Phys.* (2012) 04, 033; T. Aaltonen *et al.* (CDF Collaboration), *Phys. Rev. Lett.* **107**, 191801 (2011); V. M. Abazov *et al.* (D0 Collaboration), *Phys. Lett. B* **693**, 539 (2010); G. Aad *et al.* (ATLAS Collaboration), *Phys. Lett. B* **713**, 387 (2012).
  - [3] A. Lenz and U. Nierste, *arXiv:1102.4274*.
  - [4] R. Aaij *et al.* (LHCb Coll.), LHCb-CONF-2012-002.
  - [5] K. De Bruyn, R. Fleischer, R. Kneijens, P. Koppenburg, M. Merk, and N. Tuning, *arXiv:1204.1735* [Phys. Rev. D (to be published)].
  - [6] W. Altmannshofer, P. Paradisi, and D. M. Straub, *J. High Energy Phys.* (2012) 04, 008.
  - [7] R. Fleischer, *Phys. Rep.* **370**, 537 (2002).
  - [8] C.-S. Huang and W. Liao, *Phys. Lett. B* **525**, 107 (2002).
  - [9] A. Dedes and A. Pilaftsis, *Phys. Rev. D* **67**, 015012 (2003).
  - [10] P. H. Chankowski, J. Kalinowski, Z. Was, and M. Worek, *Nucl. Phys. B* **713**, 555 (2005).
  - [11] I. Dunietz, R. Fleischer, and U. Nierste, *Phys. Rev. D* **63**, 114015 (2001).
  - [12] T. Aaltonen *et al.* (CDF Collaboration), *Phys. Rev. D* **84**, 052012 (2011); R. Aaij *et al.* (LHCb Collaboration), *Phys. Lett. B* **707**, 349 (2012).
  - [13] CMS Collaboration, CERN-LHCC-2011-006; LHCb Collaboration, CERN-LHCC-2012-007.